

Synthesis and Structural and Functional Evaluation of a Protein Modified with a β -Turn Mimic

Fabienne Jean,[†] Eric Buisine,^{†,‡} Oleg Melnyk,[†] Hervé Drobecq,[†] Benoît Odaert,[†] Michel Hugues,[§] Guy Lippens,^{*,†} and André Tartar^{†,||}

Contribution from the Laboratoire Synthèse, Structure, Fonction des Biomolécules URA CNRS 1309, Institut de Biologie de Lille, Institut Pasteur de Lille, 1 Rue du Professeur Calmette, BP 447, 59021 Lille Cedex, France, and Laboratoire de Physiopathologie et Pharmacologie Vasculaire, Université Victor Segalen Bordeaux 2 CNRS/ESA 5017 - UFR Sciences Pharmaceutiques, 146 rue Léo Saignat, 33076 Bordeaux, France

Received July 14, 1997

Abstract: Protein engineering has traditionally relied upon the possibility of changing the primary structure by either site-directed mutagenesis or peptide synthesis. Recently the scope of these methods has been extended to non-natural amino acids by both biosynthetic and synthetic approaches. A further step in which a complete structural motif is replaced by an equivalent synthetic mimic has been validated in small peptides. We extend these results to the field of protein engineering by incorporating a β -turn mimic into a small protein, scyllatoxin, which contains all major secondary structure elements. The synthetic scyllatoxin was structurally and functionally characterized and found to be equivalent to the native protein.

Introduction

The engineering of stable, folded, and functional polypeptides has recently attracted much research attention.¹ While research has focused either on a fundamental understanding of the rules that govern protein folding^{2,3} or on its many potential applications,^{4,5} an important question remains about how the properties of individual amino acids determine which structures will form as the protein folds up into its final shape. Peptide models have largely contributed to our understanding of these rules, but it is now generally accepted that they are not absolute mimics of proteins. A particular example of this discrepancy is the simple arrangement of a β -sheet, one of the fundamental secondary-structure elements where neighboring strands often come from distant regions of the protein. However, even when the strands forming the β -sheet lie adjacent to each other along the linear

protein chain, the rules that determine β -hairpin conformation are still not fully elucidated. It is clear that the region where the chain bends, makes a significant contribution not only to the stability of the final protein but also to the kinetics of folding.² Building upon these observations, several β -turn mimics have been designed and evaluated on their capacity to nucleate β -sheets in small peptides.^{6,7} These building blocks come from organic chemistry and are used to impose a chain reversal and a correct hydrogen-bonding pattern of the directly attached amino acids. A number of them have been successfully incorporated into different model peptides, but their small size and subsequent flexibility, as well as their tendency to aggregate in aqueous solution, hamper their extensive use in the framework of this subdomain of protein chemistry. A first example where a building block replacing a complete structural element was incorporated into a full protein structure is the HIV-1 protease.⁷ However, only a weak biological activity of the resulting product was observed, and the very limited purity of the final product prevented any structural characterization.

The goal of our study was dual: first, to evaluate from a chemical, structural, and functional point of view the incorporation of a β -turn mimic into a real protein environment as defined by the existence of a full tertiary structure, and second, to obtain further insights into the mechanisms of β -sheet formation through the strategy of a mimic replacing the turn. The constraints placed upon the protein model were (i) a small size compatible with peptide synthesis and NMR analysis, (ii) the presence of the major secondary-structure elements folded into a stable tertiary structure, (iii) a solvent-exposed β -turn, and (iv) an easily detectable biological activity dependent upon the integrity of the structural organization of the protein but not directly involving the amino acids present in the β -turn.

[†] Institut Pasteur de Lille.

[‡] Faculté des Sciences Pharmaceutiques et Biologiques, Université de Lille 2, 3 rue du Professeur Laguesse, BP83-59006 Lille Cedex, France.

[§] Université Victor Segalen Bordeaux 2 CNRS/ESA 5017- UFR Sciences Pharmaceutiques.

^{||} Present address: CEREP, 1, rue du Professeur Calmette, 59201 Lille Cedex, France.

* To whom correspondence should be addressed (e-mail: Guy.Lippens@pasteur-lille.fr).

(1) (a) Muir, T. W.; Kent, S. B. H. *Curr. Opin. Biotechnol.* **1993**, *4*, 420–427. (b) Nowak, M. W.; Kearney, P. C.; Lester, H. A. *Science* **1995**, *268*, 439–442. (c) Chung, H.-H.; Benson, D. R.; Cornish, V. W.; Schultz, P. G. *Proc. Natl. Acad. Sci. U.S.A.* **1993**, *90*, 10145–10149. (d) Ellman, J. A.; Mendel, D.; Schultz, P. G. *Science* **1992**, *255*, 197–200. (e) Struthers, M. D.; Cheng, R. P.; Imperiali, B. *Science* **1996**, *271*, 342–345. (f) Vita, C.; Roumestand, C.; Toma, F.; Ménez, A. *Proc. Natl. Acad. Sci. U.S.A.* **1995**, *92*, 6404–6408. (g) Mendel, D.; Ellman, J. A.; Chang, Z.; Veenstra, D. L.; Kollman, P. A.; Schultz, P. G. *Science* **1992**, *256*, 1798–1802.

(2) (a) Garret, J. B.; Mullins, L. S.; Raushel, F. M. *Protein Sci.* **1996**, *5*, 204–211. (b) Muñoz, V.; Thompson, P. A.; Hofrichter, J.; Eaton, W. A. *Nature* **1997**, *390*, 196–199.

(3) Minor, D. L.; Kim, P. S. *Nature* **1996**, *380*, 730–734.

(4) (a) Bryson, J. W.; Betz, S. F.; Lu, H. S.; Suich, D. J.; Zhou, H. X.; O'Neil, K. T.; DeGrado, W. F. *Science* **1995**, *270*, 935–941. (b) Kahn, M.; Wilke, S.; Chen, B.; Fujita, K.; Lee, Y.-H.; Johnson, M. E. *J. Mol. Recognit.* **1988**, *1*, 75–79.

(5) Tuchscherer, G.; Mutter, M. *J. Pept. Sci.* **1995**, *1*, 3–10.

(6) (a) Kemp, D. S.; Li, Z. Q. *Tetrahedron Lett.* **1995**, *36*, 4179–4180.

(b) Nesloney, C. L.; Kelly, J. W. *Bioorg. Med. Chem.* **1996**, *4*, 739–766.

(c) Tsang, K. Y.; Diaz, H.; Graciani, N.; Kelly, J. W. *J. Am. Chem. Soc.* **1994**, *116*, 3988–4005.

(7) Baca, M.; Alewood, P. F.; Kent, S. B. H. *Protein Sci.* **1993**, *2*, 1085–1091.

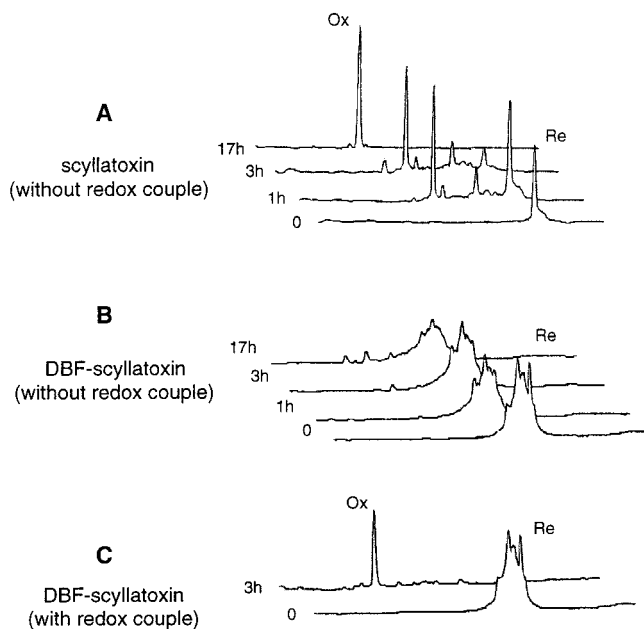


Figure 3. HPLC profiles of comparative folding experiments. Kinetics of folding of scyllatoxin (profile A) and DBF-scyllatoxin (profile B). "Re" indicates the reduced form of the toxin and "Ox" the oxidized form. (C) Folding experiment of DBF-scyllatoxin with a redox couple reduced/oxidized glutathione (4/2 mM).

formation of the chain as a consequence of the chain return imposed by DBF. The four hypotheses can lead to a decreased accessibility of the reactive amine function to the active ester.¹³

Oxidation of the peptide to form the three disulfide bridges is a straightforward procedure for the nonmodified scyllatoxin. If one works at a sufficient dilution to avoid formation of interchain disulfide bridges, a correctly folded scyllatoxin results from simple oxidation with air. Therefore, upon completion of the synthesis, the DBF-containing peptide was simultaneously cleaved from the resin and deprotected by treatment with TFA and a mixture of scavengers containing dibenzofuran to prevent a potential alkylation of the mimic¹⁴ and then oxidized according to the procedure as established for scyllatoxin. However, RP-HPLC profiles recorded at different moments revealed serious problems of aggregation (data not shown). Upon the basis of this result and the analysis of the synthesis problems, we decided to further purify the reduced peptide by preparative RP-HPLC, before attempting the oxidation. This step eliminated successfully a number of incomplete sequences, and we proceeded to the oxidation/folding step with the purified product. Under the conditions used for scyllatoxin (0.33 M NH_4HCO_3 buffer, pH 8, 4 °C, without redox couple), the oxidized product of DBF-scyllatoxin could not be obtained (Figure 3). However, the presence of the redox couple reduced/oxidized glutathione allowed its formation. These comparative oxidation experiments indicate the non-negligible role of the β -turn in the folding process. Similar results had previously been obtained upon

comparing of the folding process of different long neurotoxins: one additional amino acid in the turn region of three toxins considerably slowed their folding kinetics when compared to six other members of the family.¹⁵ Whereas the sequence divergence of the toxins could be partially responsible for this difference, the comparative refolding kinetics of one toxin and two point mutants where an additional residue was inserted in this turn region confirmed the previous results (A. Ménez, personal communication). The coexistence of more than one β -hairpin conformation and the flexibility derived from it was recently proposed to be essential for protein chains to attain the most favorable conformation compatible with a stabilizing tertiary structure.¹⁶ The rigid nature of the DBF moiety seems to hamper this sampling of conformational space, leading to a less efficient folding.

Upon completion of the oxidation, the peptide was purified by two successive purification steps by RP-HPLC as described in the Experimental Methods and analyzed by RP-HPLC, capillary electrophoresis, electrospray mass spectroscopy, and amino acid analysis.¹⁷ Eventually, 1.5 mg of the oxidized product was obtained, allowing a functional characterization and a detailed structural analysis by NMR.

Structure Determination. To evaluate the influence of the mimic on the final protein structure, a detailed NMR analysis of the molecule was performed. Resonance assignments of the backbone and side-chain protons were established by following the classical assignment procedure according to Wüthrich¹⁸ and revealed only minimal differences in $\text{H}\alpha$ and NH chemical shifts as compared with the values observed in scyllatoxin,¹⁹ indicating the structure similarity of the two peptides. The NOE analysis first confirmed the presence of the major secondary structure elements in the modified toxin: the short N-terminal β -strand and the C-terminal β -hairpin were characterized by strong sequential αN NOEs as well as by the several long-range $\text{H}\alpha$ – $\text{H}\alpha$ contacts, whereas the α -helix was clearly identified between Leu 5 and Ser 14 by the pattern of strong NH–NH($i,i+1$) contacts completed by the $\alpha\beta(i,i+3)$ contacts (data not shown). The tertiary structures of many small scorpion structures has been shown to depend critically on the presence of a glycine residue at position 16, where the α -helix crosses over the C-terminal β -hairpin.⁸ The NOE cross-peaks observed on the spectrum of the DBF-scyllatoxin between the Gly 19 NH and $\text{H}\alpha$ protons and both the $\text{H}\alpha$ proton of Gln 9 and the $\text{H}\beta$ of Cys 12 confirmed a correct packing of the secondary-structure elements into the native tertiary structure. A full analysis of the NOE contacts, J couplings, and protection factors in a H/D exchange experiment confirmed that the peptidic parts of DBF-scyllatoxin and scyllatoxin^{19,20} were very similar, with the classical motif of an α -helix linked by three disulfide bridges to a β -sheet (Figure 4A).

The average pairwise root-mean-square deviation of the peptidic backbone (residues 3–29) of the final DBF-scyllatoxin structures versus those of scyllatoxin was 1.2 Å. Therefore, we concluded that the DBF mimic is tolerated to replace the

(13) (a) Stewart, J. M.; Klis, W. A. Innovation and perspectives in solid-phase synthesis. In *Peptides, polypeptides and oligonucleotides*; Epton, R., Ed.; SPCC Ltd.: Birmingham, U.K., 1990; pp 1–9. (b) Deber, C. M.; Lutek, M. K.; Heimer, E. P.; Felix, A. M. *Pept. Res.* **1989**, *2*, 184–188. (c) Ludwick, A. G.; Jelinski, L. W.; Live, D.; Kintanar, A.; Dumais, J. J. *J. Am. Chem. Soc.* **1986**, *108*, 6493–6496. (d) Tam, J. P.; Lu, Y. A. *J. Am. Chem. Soc.* **1995**, *117*, 12058–12063. (e) Fields, G. B.; Fields, C. G. *J. Am. Chem. Soc.* **1991**, *113*, 4202–4207.

(14) A first synthesis of DBF-scyllatoxin using an automatic Boc/benzyl strategy had been attempted. RP-HPLC and TOF-PDMS analyses performed on the crude peptide just after the cleavage and deprotection step had shown the presence of DBF-containing peptide fragments being alkylated with a tBu group.

(15) Ménez, A.; Bouet, F.; Guschlbauer, W.; Fromageot, P. *Biochemistry* **1980**, *19*, 4166–4172.

(16) de Alba, E.; Jiménez, M. A.; Rico, M. *J. Am. Chem. Soc.* **1997**, *119*, 175–183.

(17) A slight shoulder on the RP-HPLC peak was observed but the corresponding product could not be isolated for identification. The ESMS spectra shows a minor peak ($M + 71$).

(18) Wüthrich, K. *NMR of Proteins and Nucleic Acids*; Wiley: New York, 1986.

(19) Martins, J. C.; Zhang, W.; Tartar, A.; Lazdunski, M.; Borremans, F. A. M. *FEBS Lett.* **1990**, *260*, 249–253.

(20) Martins, J. C.; Van de Ven, F. J. M.; Borremans, F. A. M. *J. Mol. Biol.* **1995**, *253*, 590–603.

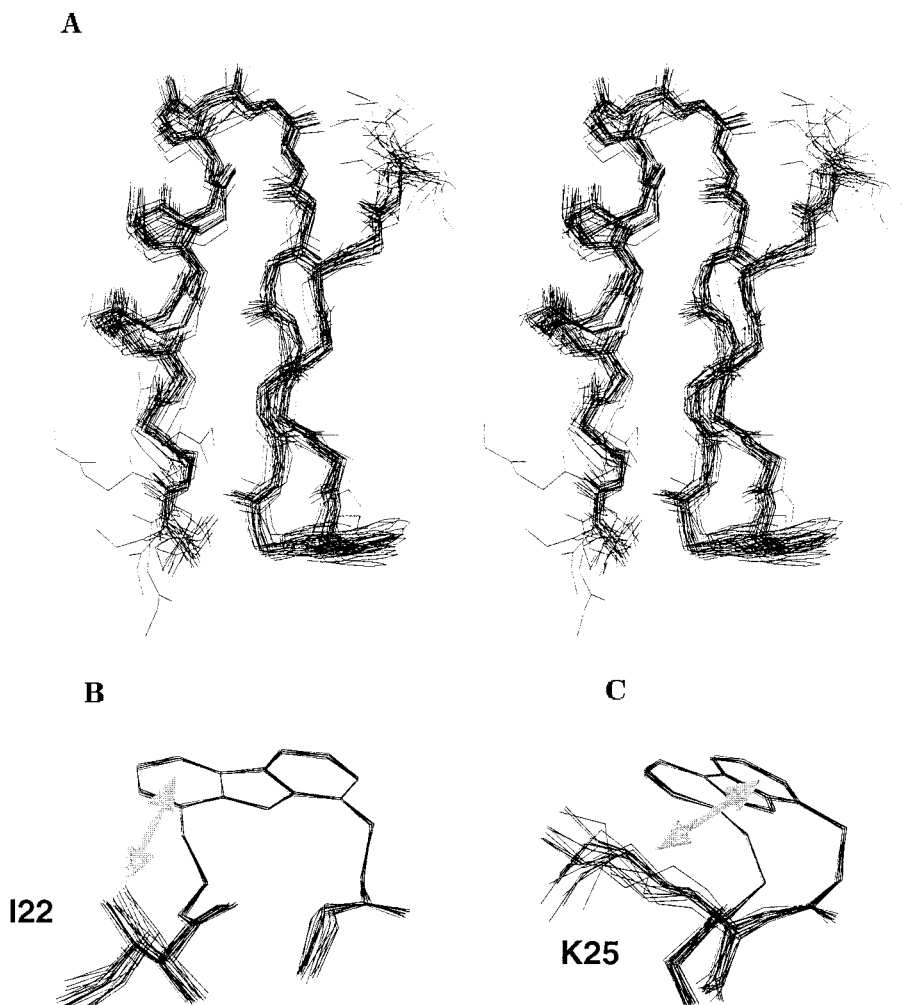


Figure 4. (A) Stereoview of the 24 final conformers of the DBF-scyllatoxin in solution. The conformers are superimposed with respect to the backbone atoms of residues 3–29 (rmsd \approx 0.76 Å). Heavy atoms of the DBF-based mimic are included in fitting. (B and C) Detailed views of the β -turn mimic region showing the hydrophobic stacking of the aromatic moiety with side chains of the flanking residues Ile 22 and Lys 25. Arrows indicate the different NOE contacts involving (B) the DBF aromatic protons H₁, H₂, and H₃ with the γ -methyl protons Ile 22 and (C) the DBF aromatic protons H₇, H₈, and H₉ with the H _{β} , H _{δ} , and H _{ϵ} protons of the Lys 25 residue.

central residues of the β -turn without disruption of the overall structure of scyllatoxin.

Several considerations led us to investigate in detail the final conformation of the DBF moiety in the protein context. Modeling studies based upon the replacement of the two central residues of the β -turn, Gly 23 and Asp 24, by stable conformations of the DBF-mimic (see the Experimental Methods) had indicated that incorporation should be compatible with the native fold. However, the hydrophobic character of the DBF group was only partially taken into account in this preliminary modeling study, owing to the lack of accurate parameters describing its interaction with the solvent. Second, Kelly et al. had put forward, as an absolute requirement for the mimic to nucleate a β -sheet, the presence of a hydrophobic cluster or π -cation-like interactions with the side chains of the flanking residues.^{1f,21} In the context of small designed peptides, this requirement proved to be a stringent selective criterium on the nature of the flanking residues. Whereas Ile 22 clearly fulfills this role in the scyllatoxin sequence, it was not clear what the behavior of the Lys 25 side chain would be. Rather than replacing this side chain by a hydrophobic one, we decided to maintain the native lysine residue. Resonance assignments for

Ile 22 and Lys 25 protons indicated a clear upfield shift in the case of DBF-scyllatoxin as compared to scyllatoxin¹⁹ (values indicated in parentheses), with the most dramatic effect for Ile 22 methyl groups and the Lys 25 β and γ methylene protons: Ile 22, NH 8.82 (9.06), H α 4.07 (4.31), H β 1.04 (1.81), γ CH₃ 0.11 (0.86), δ CH₃ 0.31 (0.76); Lys 25, NH 7.77 (7.77), H α 4.43 (4.50), H β 0.96 (1.82), γ CH₂ 0.10, 0.47 (1.39), δ CH₂ 1.34 (1.67), ϵ CH₂ 2.63 (3.00). Moreover, careful inspection of the NMR spectra revealed NOE contacts between the side chains of Ile 22 and Lys 25 with the DBF aromatic protons: the γ methyl group of Ile 22 interacts with the H₁, H₂, and H₃ protons of the DBF group, while the H β , H δ , and H ϵ protons of Lys 25 take contacts with the H₇, H₈, and H₉ aromatic protons. Both classes of NOE contacts confirm the efficient stacking of the DBF with both side chains (Figure 4B,C).

CD Spectra of the Native and Modified Scyllatoxin. The far-UV CD spectra of scyllatoxin and DBF-scyllatoxin are qualitatively similar (Figure 5). They both display the characteristics of CD spectra of folded proteins with a maximum at 192 nm and two characteristic minima at 207 and 222 nm. As the NMR analysis confirms the structural conservation of the toxin after the DBF insertion, the difference of shape between the two CD curves in the region of 207–240 nm probably

(21) Graciani, N. R.; Tsang, K. Y.; McCutchen, S. L.; Kelly, J. W. *Bioorg. Med. Chem.* **1994**, *2*, 999–1006.

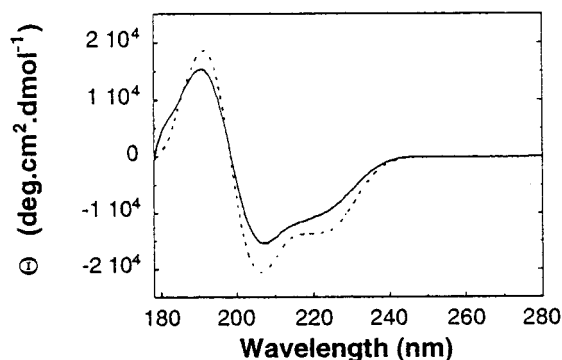


Figure 5. Far-UV CD spectra of scyllatoxin (—) and DBF-scyllatoxin (---) at 4 °C in an aqueous solution at pH 5.

originates from the aromatic contribution of the dibenzofuran in its rigid asymmetric environment.

Comparative Stabilities of the Native and Modified Scyllatoxin. To test the effect of the DBF insertion on the protein stability, comparative denaturations by temperature, urea, and pH were attempted. For temperatures ranging from 5 to 85 °C, no drastic changes in the CD spectra of both native scyllatoxin and DBF-scyllatoxin were observed, and similar results were obtained when we tried to denature both proteins by increasing urea concentrations or acidic pH (data not shown). Neither a 6 M urea concentration or a pH of 1 was capable of denaturing any of the molecules. The extreme stability of the short toxins, however, is known to depend critically on the presence of the disulfide bridges.⁸ We therefore tested the stability of the molecules by thermal denaturation studies in the presence of an excess of the reducing agent TCEP (Figure 6A,B). As supported by the appearance in the CD spectra of a minimum at 200 nm and the disappearance of the minimum at 222 nm on CD spectra, both proteins were totally unfolded after treatment above 65 °C. Compared to the native protein, the DBF-scyllatoxin seems to be less stable, with a 15 °C decrease in the apparent T_m . The presence of an isodichroic point at 202 nm points toward a two-state model. However, the irreversible character of the unfolding reaction indicates that the experiment does not probe the equilibrium populations at a given temperature, but rather the kinetics of disulfide reduction and subsequent protein unfolding. Therefore, we compared these kinetics in the presence of TCEP at 37 °C (Figure 6C). In agreement with a two-state model, the decay for both molecules could be fitted successfully to a monoexponential curve, with a rate of unfolding of the DBF-scyllatoxin that is 3 times faster than that for scyllatoxin. While both CD experiments indicate that the organic mimic does influence the accessibility of the reducing agent to the core of the molecule, the surprising result is that it does not protect the protein core, but renders it more accessible to the reducing agent.

Biological Activity. The activity of scyllatoxin depends critically upon the correct positioning in space of several side chains in the α -helix and in the C-terminal section of the molecule²² and forms an extremely sensitive probe of 3D structuration. Biological and biochemical activities were therefore compared for scyllatoxin and DBF-scyllatoxin in (i) an isometric contraction measurement in guinea pig *Taenia coli* being directly dependent upon scyllatoxin blocking of the low-conductance calcium-dependent potassium channels^{22–24} (Figure 7A,B) and (ii) comparative competition experiments between

[¹²⁵I]apamin and scyllatoxin or DBF-scyllatoxin on rat brain membrane preparation^{22,24} (Figure 7C,D). The comparable activities in the tests for both molecules confirmed the structural integrity of the DBF-scyllatoxin, as well as the correct orientation of the relevant side chains.

Conclusion

Although it is not obvious that our results can be extended unconditionally to every β -turn found in other protein sequences, the DBF-scyllatoxin molecule described in this report indicates the feasibility of replacing a secondary-structure element composed of several residues by a well-designed mimic. The result of the decreased stability after insertion of the DBF mimic was surprising to us and has motivated us to incorporate the DBF molecule in a second protein model, the B1 domain of protein G, where the absence of cysteine residues should alleviate the difficulties encountered in the unfolding study of the DBF-scyllatoxin.

Our present results confirm the importance of evaluating structural modifications in a full-protein context, rather than limit oneself to various peptide models. Whereas the role of the charged lysine side chain in the formation of a hydrophobic cluster during the oxidation and folding process cannot be inferred from the final structure, the latter does extend the results previously obtained upon incorporation of the mimic in small designed peptides. Finally, the full characterization at both the structural and functional level of the modified toxin reveals that organic chemistry has indeed entered the realm of protein engineering.

Experimental Methods

Material and Methods. Fmoc amino acids derivatives, Rink amide resin (4-((2',4'-dimethoxyphenyl)-Fmoc-aminoethyl)phenoxy resin), and PyBrop were purchased from Novabiochem (EMA, Meudon, France). HBTU and BOP were obtained from Propeptide (Vert-Le-Petit, France), and HOBt was from Acros (Geel, Belgium). Piperidin, DIEA, TFA, acetic anhydride, guanidine hydrochloride, reduced and oxidized glutathione, ethanedithiol, thioanisole, and phenol was purchased from Aldrich (Steinheim, Germany). *N,N*-Dimethylformamide (Carlo Erba, Val de Reuil, France), after addition of aluminum oxide (type 504C, pH 4.5, Fluka, Buchs, Switzerland), was filtered and stored on 4-Å molecular sieves.

Preparative and analytical HPLC were performed on a Shimadzu system. Analytical HPLC was run on a Nucleosil C18 column (300 Å, 7 mm, 4.6 mm \times 25 cm) at a flow rate of 1 mL/min. Preparative HPLC was run on a Nucleosil C18 column (100 Å, 5 mm, 1 cm \times 50 cm) at a flow rate of 2 mL/min and on a Nucleosil CN column (100 Å, 5 mm, 1 cm \times 50 cm) at a flow rate of 2 mL/min. All runs were linear gradients of 0.05% aqueous TFA versus 60% acetonitrile 0.05% TFA.

Capillary electrophoresis experiments were performed on an Applied Biosystems model 270A apparatus. The peptides were analyzed by TOF-PDMS mass spectrometry (BioIon) and electrospray mass spectroscopy on an API simple-quadrupole mass spectrometer (Perkin-Elmer-Sciex) equipped with an ion-spray (nebulizer-assisted electrospray) source. Amino acids analyses were performed on a Beckman model 6300 amino acids analyzer.

Synthesis of the Dibenzofurane-Based β -Turn Mimic. The synthesis was performed according to the protocole previously published by Kelly and co-workers.^{1f} The Fmoc derivative of **1** was prepared from 1.90 g (4.96 mmol) of the *tert*-butyloxycarbonyl (Boc)-protected analogue of **1** by cleavage of the Boc group with TFA (118.4 mL) in 52 mL of dichloromethane. The amine function was then protected

(22) Auguste, P.; Hugues, M.; Mourre, C.; Moinier, D.; Tartar, A.; Lazdunski, M. *Biochemistry* **1992**, *31*, 648–654.

(23) Hugues, M.; Duval, D.; Schmid, H.; Kitabgi, P.; Lazdunski, M.; Vincent, J.-P. *Life Sci.* **1982**, *31*, 437–443.

(24) Auguste, P.; Hugues, M.; Gruvé, B.; Gesquière, J.-C.; Maes, P.; Tartar, A.; Romey, G.; Schweitz, H.; Lazdunski, M. *J. Biol. Chem.* **1990**, *265*, 4753–4759.

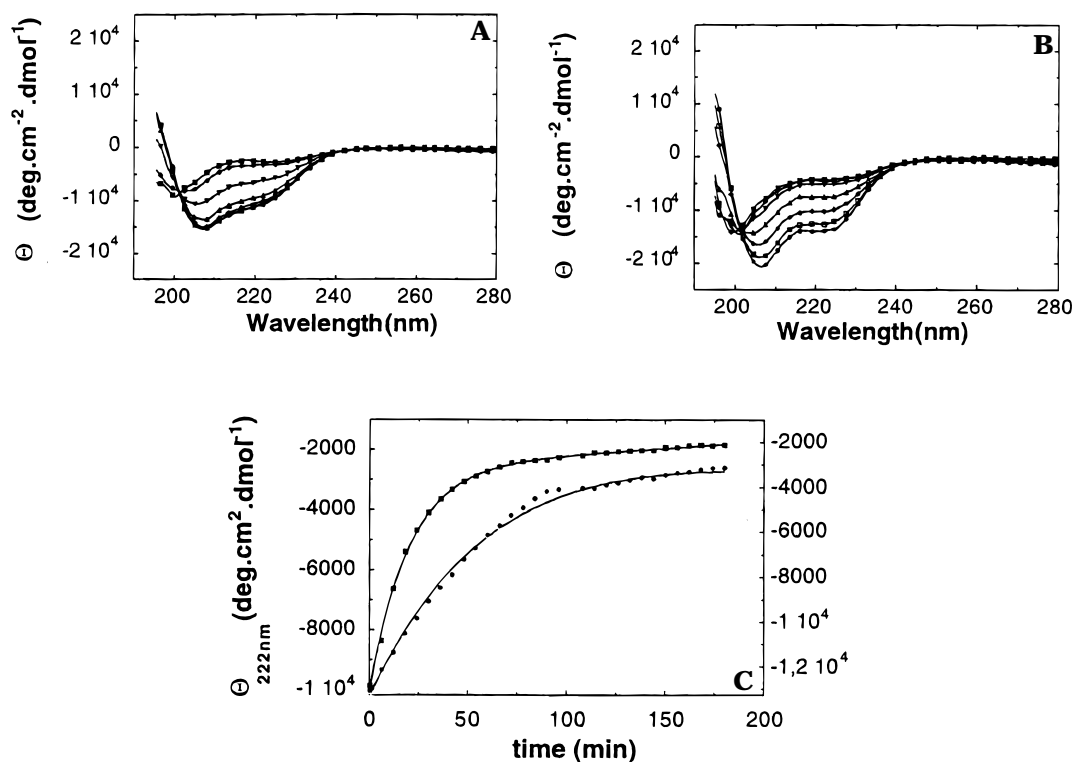


Figure 6. Thermal denaturations of scyllatoxin (A) and DBF-scyllatoxin (B) upon disulfide bridge reduction in the presence of an excess of TCEP. The far-UV CD spectra were successively acquired at 5 °C (●), 15 °C (□), 25 °C (◆), 35 °C (Δ), 45 °C (▼); 55 °C (◇), and 65 °C (■). In panel C, the unfolding kinetics of scyllatoxin (●, left) and DBF-scyllatoxin (■, right) upon reduction were extracted from the CD spectra recorded at 37 °C every 6 min and were fitted by a monoexponential function to give respectively rate constants of 1 and 3 h⁻¹.

by reaction with 2.45 g (7.26 mmol) of Fmoc-hydroxysuccinimide in the mixture H₂O/acetone (35 mL/20 mL) and addition of Na₂CO₃ to maintain the pH around 9. After 3 h, the pH was altered to pH 1–2 with 1.2 N HCl. The product was then extracted with EtOAc and dried over Na₂SO₄, and the solvents were evaporated under vacuum. Due to its poor solubility in solvents, the Fmoc derivative of **1** was purified by trituration in dichloromethane to afford 1.79 g (88%) of the product.

¹H NMR (300 MHz, CDCl₃): δ 7.81 (m, 4 H, Ar-1,9 H and Ar-1',9' H), 7.36 (m, 10 H, Ar-2,3 H and Ar-2',3' H), 4.44 (d, $J = 6.8$ Hz, 1 H, NH), 3.70 (m, 2H, CH₂NH), 3.42 (m, 2H, ArCH₂CH₂), 3.23 (m, 2H, ArCH₂). Mass spectrometry: m/z (M^+) calcd 505.6; obsd 544.4 ($M + K$), 528.4 ($M + Na$).

Solid-Phase Peptide Synthesis. The DBF-scyllatoxin was synthesized manually by solid-phase peptide synthesis. Rink amide resin having a loading of 0.47 mmol/g was used and different coupling agents depending on coupling difficulty: HBTU/HOBt, BOP, PyBrop. Fmoc-protected amino acids had the following side-chain protections: *tert*-butyl ether (tBu) for Ser; *tert*-butyl ester (OtBu) for Glu; trityl (Trt) for Cys and His; 2,2,5,7,8-pentamethylchromane-6 sulfonyl (Pmc) for Arg; Boc for Lys; methyltrityl (Mtt) for Asn and Gln.

For activation, 2 mmol of amino acid was dissolved in 4 mL of 0.45 M HBTU/HOBt solution (1.8 mmol) in DMF and 8 mmol of DIEA. After 3 min, the coupling solution was added to 0.5 mmol of Rink amide resin. The resin was vortexed for 30 min. When TNBS test or ninhydrin test remained positive, another coupling was performed using HBTU/HOBt or BOP or PyBrop, with the same stoichiometry, before capping with acetic anhydride 10% in dichloromethane (10 min). The multiple couplings were as follows: His 31 to Cys 26, two couplings HBTU/HOBt; Lys 25, Ile 22, three couplings HBTU/HOBt; Cys 21, two couplings HBTU/HOBt; Lys 20, three couplings HBTU/HOBt; Gly 19, two couplings HBTU/HOBt; Leu18 to Leu 10, three couplings HBTU/HOBt (temperature increased to 40 °C: Leu15 to Cys 12); Gln 9, fifth coupling: BOP; Cys 8, third coupling PyBrop; Met 7, second and fourth couplings PyBrop; Arg 6, third coupling PyBrop, fourth coupling BOP; Leu 5, three couplings BOP; Asn 4, two couplings BOP, third coupling PyBrop; Cys 3 to Phe 2, two couplings BOP; Ala 1, two couplings BOP, third coupling PyBrop.

The coupling of the β -turn mimic **1** (Fmoc derivative) was performed using 1.3 equiv of the mimic, 1.2 equiv of HBTU/HOBt, and 3.3 equiv of DIEA in DMF for the first coupling. For second and third couplings, PyBrop was used in place of HBTU/HOBt.

Deprotection of the Fmoc group was performed by two successive 12-min treatments with 20% piperidine in DMF, except for deprotection of Gly 19 (four piperidine treatments), Leu 18 to Gly 16 and Ser 11 (three piperidine treatments) and at 40 °C from Gly 16 to Arg 13. After completion of the last cycle, the resin was washed with ethanol and ether and dried in vacuo. The peptide was simultaneously cleaved from the resin and deprotected by treatment with TFA (10 mL), H₂O (500 mL), phenol (750 mg), ethanedithiol (250 mL), thioanisole (500 mL), and dibenzofuran (380 mg). After stirring at room temperature for 3 h, the resin was filtered and the solution was added dropwise to diethyl ether to precipitate the peptide. After 5 min of centrifugation at 3000 rpm, the peptide pellet was resuspended in diethyl ether and the process repeated twice. The final pellet was dried under nitrogen and dissolved in 6 M guanidine hydrochloride. The peptide was then prepurified before disulfide formation.

Disulfide Bridge Formation and Purification. The crude peptide was first prepurified by preparative RP-HPLC on a Nucleosil C18 column. The peptide was eluted at a 2 mL/min flow rate with a 1-h 12–42% acetonitrile gradient in 0.05% TFA. The fractions were checked using capillary electrophoresis and TOF-PDMS, pooled, and lyophilized.

The prepurified peptide was dissolved in 500 mL of TFA and added dropwise to the oxidation solution (final peptide concentration 10⁻⁵ M) containing NH₄HCO₃ (0.33 M final pH = 8), 4 × 10⁻³ M reduced glutathione, and 2 × 10⁻³ M oxidized glutathione.

After 17 h of stirring at 4 °C, the oxidation solution was acidified to pH 2 with TFA and then directly applied to the preparative RP-HPLC Nucleosil C18 column at a 5 mL/min flow rate. The peptide was then eluted at 2 mL/min with a 60-min 18–39% acetonitrile gradient in 0.05% TFA. Fractions containing the oxidized peptide were analyzed by capillary electrophoresis and TOF-PDMS, pooled, and lyophilized before the last purification step on a Nucleosil CN column, using a 90-min 12–30% acetonitrile gradient in 0.05% TFA at a 2

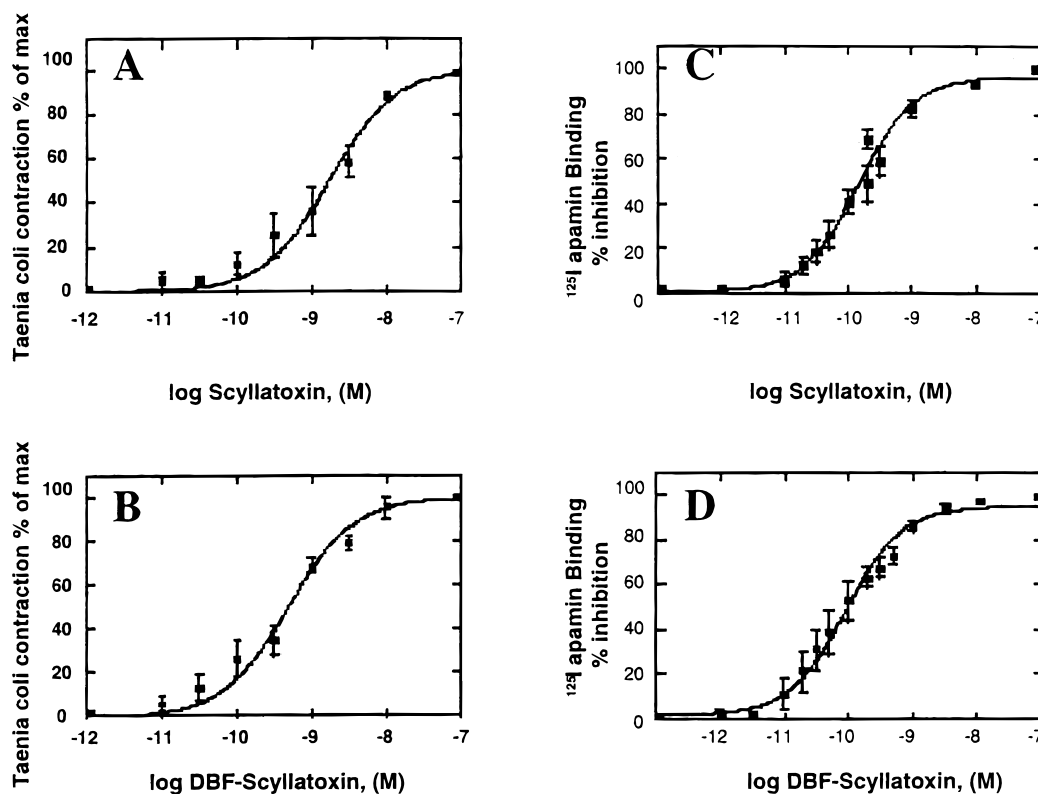


Figure 7. Biological (A and B) and pharmacological (C and D) potencies of scyllatoxin and DBF-scyllatoxin. Measurement of the isomeric contraction of a guinea pig *T. coli* induced by scyllatoxin (A) or DBF-scyllatoxin (B). Both toxins were found to exhibit comparable contractile activities as demonstrated by curves in panel A (scyllatoxin, IC_{50} 173 pM \pm 37 ($n = 3$)) and B (DBF-scyllatoxin, IC_{50} 48 pM \pm 6 ($n = 3$)). Competition experiments between scyllatoxin (C) and DBF-scyllatoxin (D) with [125 I]apamin on rat brain membrane preparation. IC_{50} 's were found to be 145 pM \pm 20 for scyllatoxin ($n = 3$) (C) and 90 pM \pm 14 for DBF-scyllatoxin ($n = 3$) (D). IC_{50} 's values for scyllatoxin and DBF-scyllatoxin were in good agreement with previously published values for scyllatoxin.

mL/min flow rate, to afford 1.5 mg of the product after lyophilization. The peptide was then characterized by ESMS and amino acids analysis. ESMS: obsd, 3517.7 \pm 0.3 Da; calcd for $C_{153}H_{244}N_{44}O_{37}S_7$, 3517.0 Da. The amino acid composition of the peptides during the synthesis were analyzed after hydrolysis of peptidyl-resin samples with 0.5 mL of 12 M HCl, 0.5 mL of propionic acid, and 20 mL of 5% (by mass) phenol in H_2O at 140 $^{\circ}C$ for 3 h *under vacuum*. The amino acid composition of the purified peptide was analyzed after hydrolysis with 1 mL of 6 M HCl and 20 mL of 5% phenol (by mass) in H_2O at 110 $^{\circ}C$ for 24 h *under vacuum*. Amino acid analysis for DBF-scyllatoxin: Asx(1) 1.0, Ser(2) 2.0, Glx(2) 2.4, Gly(2) 2.3, Ala(1) 1.1, Cys(6) 5.4, Val(1) 1.0, Met(1) 0.7, Ile(1) 0.7, Leu(5), 5.1, Phe(1) 0.9, His(1) 1.0, Lys(3) 3.0, Arg(2) 2.0.

CD Studies. Far-UV CD spectra of scyllatoxin and of DBF-scyllatoxin were recorded on a Jobin & Yvon spectrometer. Spectra were acquired at 4 $^{\circ}C$ from 178 to 280 nm with a 0.5-nm increment by using a 0.5-mm path cell. Solutions were degassed under He atmosphere prior to acquisition. Protein concentrations were determined at 50 mM by amino acid analysis. For the denaturation experiments, spectra were recorded from 5 $^{\circ}C$ to 85 $^{\circ}C$ in steps of 10 $^{\circ}C$ and back to 5 $^{\circ}C$. Stability toward acidic pH was tested by adjusting the pH between 1 and 5, as obtained by adding small amounts of concentrated HCl. Urea was added in steps of 1 M to a final concentration of 6 M. Thermal denaturations were also done in the presence of a reducing agent of disulfide bridges. The tris(2-carboxyethyl)phosphine (TCEP) was chosen for its irreversible action and its activity at acidic pH to reduce the scrambling due to the thiol–disulfide exchange reactions. An excess of TCEP (130 equiv of TCEP/disulfide bridge) was added to get a final concentration of 20 mM TCEP in a 200 mM NaH_2PO_4 aqueous solution at pH 4. Spectra were recorded from 5 to 65 $^{\circ}C$ every 10 $^{\circ}C$ and back to 5 $^{\circ}C$ to test the reversibility of the thermal denaturation process. The temperature raise was achieved in about 3 h. A second experiment used the same excess of TCEP at one given temperature of 37 $^{\circ}C$, and the time evolution was probed by CD.

Molecular Modeling. The DBF-based mimic under its *N*-acetyl and *C*-carboxamide form was used for the initial modeling study. Six low-energy conformations (CVFF force field²⁶) were selected upon the basis of the following geometrical criteria: (i) an O(*N*-acetyl)–HN-(*C*-carboxamide) distance lower than 2.5 \AA (in correspondence with the hydrogen bond between Ile 22 (CO) and Lys 25 (HN) in scyllatoxin (Brookhaven Protein Data Bank: file name 1scy), (ii) the angle between the two planes defined by the CONH functions varied between 80 $^{\circ}$ and 180 $^{\circ}$, and (iii) the distance separating the carbon atoms of the *N*-acetyl and *C*-carboxamide methyl groups varied from 4 to 6 \AA , relative to the distance between Ile 22 (C_{α}) and Lys 25 (C_{α}) in scyllatoxin. Replacement of the two β -turn residues Gly 23 and Asp 24 by the different DBF conformations demonstrated the compatibility of insertion.

NMR Structure Determination. NMR assignment followed the classical strategy¹⁸ based on homonuclear 2D NOESY, DQFCOSY, and TOCSY spectra recorded at 600 MHz. Sample conditions were 1 mM protein concentration in 500- μ L aqueous conditions at pH 4.9. NMR experiments were performed on a DMX Bruker 600-MHz spectrometer at 277 and 310 K. Unambiguous assignments of the different side-chain protons of Ile 22 and Lys 25 were obtained from a 1H – ^{13}C HSQC spectrum at natural abundance obtained on a 1 mM DBF-scyllatoxin sample in a 8-mm tube.

The structure determination proceeded in two steps. First, the peptidic part was derived upon the basis of the experimental NOE and *J* coupling constraints using a combined distance geometry and simulated annealing protocol as implemented in X-PLOR.²⁷ Constraints consisted of 201 intra-proteic (53 were intra-residual, 78 sequential, 40 medium range, and 30 long range). In addition, we used 18 distance

(25) Auguste, P.; Hugues, M.; Borsotto, M.; Thibault, J.; Romey, G.; Coppola, T.; Lazdunski, M. *Brain Res.* **1992**, 599, 230–236.

(26) Biosym Technologies, 968 Scranton Road, San Diego, CA 92121.

(27) Brüger, A. T. *X-PLOR version 3.1 manual*; Yale University: New Haven, CT, 1992.

restraints for nine hydrogen bonds inferred from slowly exchanging amide protons in a H/D exchange experiment²⁸ and 27 dihedral constraints (19 backbone ϕ angles and 8 side-chain χ_1 angles). In the 25 resulting protein structures, in a second phase, the six low-energy conformations of the DBF-based mimic were incorporated. After discarding the sterically incompatible structures, the 120 remaining conformations were subjected to a simulated annealing temperature of 1000 K followed by a slow cooling to room temperature and a restrained energy refinement with the CVFF force field. For this last step, the 246 intra-protein constraints were completed with 8 intra-mimic and 13 protein-mimic constraints.

Determination of Biochemical and Pharmacological Activity.

Biological activity was assessed by a biological assay consisting of a measurement of the isometric contraction of guinea pig *T. coli* induced by scyllatoxin as previously described.^{22,24,29} Briefly, a sample of *T.*

coli was bathed in a thermostated measurement chamber with Mac Evens buffer: (mM) 130 NaCl, 5.6 KCl, 2 CaCl₂, 0.24 MgCl₂, 11 glucose, 8 Hepes at pH 7.4 supplemented with 0.15 mM atropine, 2 mM guanethidine, and gassed with O₂/CO₂ (95/5). The *T. coli* was relaxed by addition of 3 mM epinephrine, and different concentrations of the tested toxins were added.

Scyllatoxin and DBF-scyllatoxin were also compared with respect to their biochemical activities in competition experiments between scyllatoxin, DBF-scyllatoxin, and [¹²⁵I]apamin for binding to rat brain microsomal membranes as previously described.^{22,25,29}

Acknowledgment. We thank J.-M. Wieruszski for excellent assistance with the NMR experiments and Prof. A. Ménez (CEA, France) for fruitful discussions. The 600-MHz facility used in this study was funded by the European Community (FEDER), the Région Nord – Pas de Calais (France), the CNRS, and the Institut Pasteur de Lille. Part of this work was financed by EU Grant BIO4-CT97-2086.

JA972346O

(28) Englander, S. W.; Mayne, L. *Annu. Rev. Biophys. Biomol. Struct.* **1992**, *21*, 243–265.

(29) Hugues, M.; Duval, D.; Kitabgi, P.; Lazdunski, M.; Vincent, J.-P. *J. Biol. Chem.* **1982**, *257*, 2762–2769.